International Congress Motor Vehicles & Motors 2012

Kragujevac, October 3rd-5th, 2012

MVM2012-030

Nenad Miljić[1]
Miroljub Tomić[2]
Slobodan J. Popović[3]
Marko Kitanović[4]
Predrag Mrđa[5]

Comparative Study on Combustion Features Extraction Methods in IC Engines Using Neural Networks Models

ABSTRACT: The in-cylinder pressure analysis provides important information on the combustion process and stands as an invaluable tool in the internal combustion engine research & development. Its implementation in a combustion control algorithms appears as a promising solution for attaining optimal combustion control in IC Engines. The pressure sensor durability, accuracy and price, along with increased demand for the processing power of Engine ECU, seems to be the main obstacles for putting these concept in IC engines on serial production line. This paper deals with the potentials of Artificial Neural Networks (ANN) and their application in combustion features extraction, based on the crankshaft angular speed measurements. High speed processing capabilities and acceptable accuracy of ANN make them good candidates to become a core component of the future combustion control algorithms. An radial basis function (RBF) ANN and a local linear Neuro-fuzzy model (LLNFM) are compared in order to gain some conclusions on optimal network topology, best suited for job of extracting crucial combustion features on common ECU platforms.

KEYWORDS: engine combustion analysis, neural networks, spark advance, crankshaft dynamics

INTRODUCTION

The dominant propulsion technology of the present is the internal combustion engine and it will be hardly possible to be completely replaced in the upcoming decades. Relying on fossil fuels IC Engines, in road transport, are responsible for a significant share in the of the world's CO2 emission of almost 20% [1]. The ever increasing energy demand followed by pollutant emission increase urges for more efficient powertrain solutions. The main focus of the research in the field of IC Engines is, more than ever, focused on its efficiency improvement and emission reduction toward fulfilment of CO2 targets already defined in regulatory frameworks worldwide [2].

The efficiency of the today's IC Engine is close to 80% of the thermodynamically ideal engine. Higher efficiencies are hardly achievable since the real engine process is influenced by unavoidable phenomena like heat losses, finite combustion duration, exhaust and blowdown losses, crevice effects, leakage and incomplete combustion [2]. Comprehensive study of the factors influencing the extraction of maximum useful work from the IC engine working cycle can be achieved through exergy (availability) analysis. A survey, done by Rakopoulos [4], on publications

[1] *Nenad Miljić, Research and Teaching Assistant, Internal Combustion Engines Department, Faculty of Mechanical Engineering, University of Belgrade, Kraljice Marije 16, 11120 Belgrade 35, Serbia, nmiljic@mas.bg.ac.rs*
[2] *Miroljub Tomić, Professor, Internal Combustion Engines Department, Faculty of Mechanical Engineering, University of Belgrade, Kraljice Marije 16, 11120 Belgrade 35, Serbia, mtomic@mas.bg.ac.rs*
[3] *Slobodan J. Popović, Research and Teaching Assistant, Internal Combustion Engines Department, Faculty of Mechanical Engineering, University of Belgrade, Kraljice Marije 16, 11120 Belgrade 35, Serbia, spopovic@mas.bg.ac.rs*
[4] *Marko Kitanović, Research Assistant, Internal Combustion Engines Department, Faculty of Mechanical Engineering, University of Belgrade, Kraljice Marije 16, 11120 Belgrade 35, Serbia, mkitanovic@mas.bg.ac.rs*
[5] *Predrag Mrđa, Research Assistant, Internal Combustion Engines Department, Faculty of Mechanical Engineering, University of Belgrade, Kraljice Marije 16, 11120 Belgrade 35, Serbia, pmrdja@mas.bg.ac.rs*

concerning the application of the second-law of thermodynamics to IC engines, gives detailed insight on parameters and strategies which could lead to efficiency increase by minimising exergy destruction. Some of the factors, influencing the engine efficiency, are related to engine control parameters which leave some space for efficiency improvement by implementation of more sophisticated control algorithms.

The spark advance is one of the key parameters in the SI engine performance. Phasing the start of combustion influences the combustion process itself and largely influences the amount of work which can be extracted from the working cycle. Maximum brake torque (MBT) can be achieved by optimally phasing the combustion process i.e. by setting the optimal spark advance angle. Bargende [3] showed that the optimal spark advance is closely related to the angular position of the 50% mass fraction burned (MFB50) i.e. that optimal spark advance sets the MFB50 to 8-10° CA after TDC. Mostly supported by experimental work and numerous testing, this conclusion has a logical theoretical background. Beccari [4] gave detailed explanation for the optimal position of MFB50, relying on the analysis of the minimal entropy change during combustion. He concluded that the optimal phase of the combustion process i.e. combustion start angle depends mostly on the intensity of the heat and friction losses and the rate of the heat release (ROHR) curve symmetry.

The concept of combustion indicator based spark advance control is explained in Figure 1. The figure shows an example of measured in-cylinder pressure and its numerical derivatives – ROHR and MFB, within the angle frame of the combustion process. The presented example shows a cycle where the combustion process needs to be retarded, since the MFB50 indicator is out of the wanted, optimal angular span (8-10º CA ATDC). Asymmetry of the ROHR curve, which is represented by its centroid position w.r.t. combustion duration midpoint, has an additional influence on the spark advance correction.

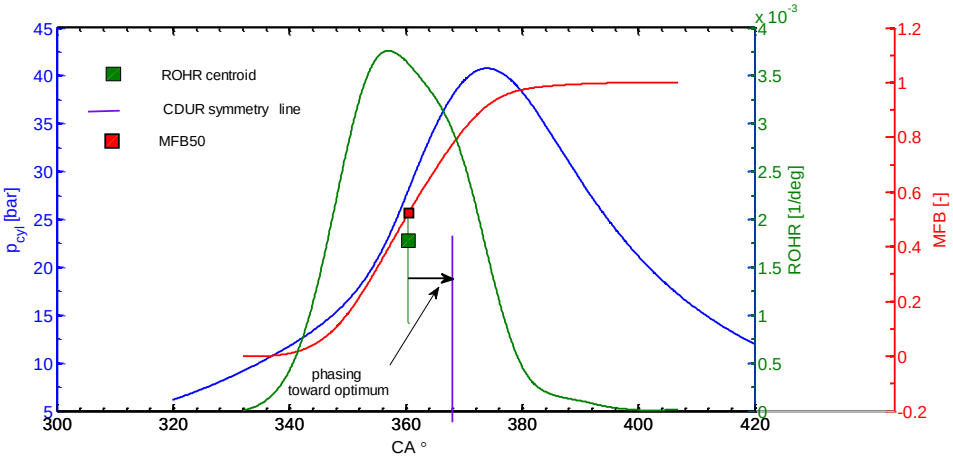

Figure 1 An example of the bad positioned combustion process which needs to be retarded in order to improve the cycle brake thermal efficiency

The relation between the MFB50 position and spark advance angle is not straightforward. By changing the start of combustion angle, thermodynamic circumstances within the combustion chamber are changing also, thus affecting the whole combustion process. That means that the phasing of the spark advance causes not only the change in ROHR curve angular position but its shape too. Therefore an advanced spark advance control system requires the feedback from the combustion process in order to maintain the highest achievable efficiency in real-time.

Today's SI engine control ignition system is map based and driven in open loop. These maps are defined through the optimisation process of the engine control parameters. Although this calibration process is very sophisticated and advanced, this open-loop type of control is unable to deliver the full efficiency potential through the engine lifetime. This is mainly caused by various influences which cannot be counted for during map calibration phase. Modern concepts, of the spark advance control, need highly accurate feedback information from the combustion process in order to achieve optimal combustion efficiency. Therefore, they urge for some kind of sensor which will provide the information on some crucial combustion features through its indicators. A combustion indicator, like MFB50, can be easily estimated from measured in-cylinder pressure. Whereas straightforward in extracting combustion features, this method has a major drawback in the pressure sensor implementation costs and its durability.

Alternative approaches are vastly investigated by researchers focusing on already available, common signals on SI engine. Among them, the angular speed and acceleration of the crankshaft has drawn far more attention because of its availability through a common engine speed measurement system. An angular speed of a crankshaft, which varies through a single engine cycle, is mainly formed by summing action of the gas torque T_g, originating from the in-cylinder gas pressure forces, and the mass torque T_m, caused by the oscillating parts of the engine. The information on the combustion process is contained in the gas torque and, consequently in the crankshaft angular speed. Although informative, the main obstacle in using the angular speed, as an effective combustion indicator

source, is the high nonlinear influence of the mass torque which can largely mask the information on the combustion process.

The crankshaft is a complex and not an absolutely stiff object, subjected to highly variable load. This lead to torsional oscillations of the crankshaft segments and, depending on the angular speed sensor placement, measured signal can be heavily influenced by this phenomenon, also.

This paper deals with the two step approach for obtaining the combustion indicator from the angular speed measurements. Relaying on relations between torques acting on the crankshaft, through the torque balance equation, first step transforms the angular acceleration to, so called, synthetic signal by freeing the original signal from mass torque influence. The second step is based on radial basis function ANN or local linear Neuro-fuzzy model (LLNFM) which uses this created synthetic signal as an input for a direct reconstruction of the MFB curve or MFB50 combustion indicator only. Thus, this method has potential to directly provide the closed loop spark advance control system with the MFB50 combustion indicator solely by measuring the angular speed of the crankshaft. Complete closed-loop control, with synthetic torque evaluation step, is presented in the Figure 2.

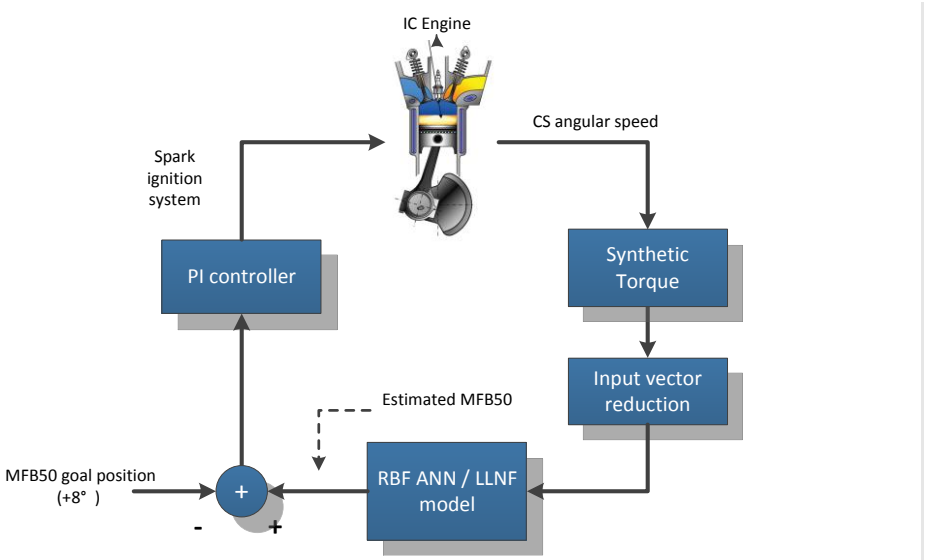

Figure 2 *Two-step concept of closed loop spark advance control implementing virtual neural network structure based MFB50 sensor*

SYNTHETIC TORQUE ESTIMATION

Crankshaft angular acceleration is built up by summing action of several torques: the gas and mass torques ($\boldsymbol{T_g}$ and $\boldsymbol{T_m}$), friction torque $\boldsymbol{T_f}$ and load torque $\boldsymbol{T_l}$. The friction torque $\boldsymbol{T_f}$ originates from the friction forces within the engine and the load torque $\boldsymbol{T_l}$ acts as an external load opposing the effective torque generated by the engine. This torques are related through the torque balance equation, which in general, for single cylinder takes form:

$$J\ddot{\theta} = T_g(\theta) + T_m\left(\theta, \dot{\theta}, \ddot{\theta}\right) + T_f(\theta) + T_l(\theta) \tag{1}$$

where θ is the crank angle and J denotes the crankshaft's moment of inertia. Information on combustion process is nested in in-cylinder pressure which is part of the gas torque T_g:

$$T_g(\theta) = p_g(\theta) \cdot A_p \cdot \frac{ds}{d\theta} \tag{2}$$

where $p_g(\theta)$ is the in-cylinder absolute pressure, A_p is the piston area and s denotes the piston displacement.
The mass torque evaluation is often based on the analysis of the kinetic energy of crankshaft mechanism modelled as two point mass system:

$$T_m\left(\theta, \dot{\theta}, \ddot{\theta}\right) = \left(-J_A(\theta) + m_B r^2\right) \cdot \ddot{\theta} - \frac{1}{2} \cdot \frac{dJ_A(\theta)}{d\theta} \cdot \dot{\theta}^2 \tag{3}$$

where the $J_A(\theta)$ is varying inertia of oscillating mass m_A w.r.t. the crankshaft axis and m_B denotes the rotating mass on crankshaft side. The exact expressions for the varying inertia and the derivatives of the piston displacement can

be found in [5]. Nonlinearity, introduced by T_m into the equation (1) is one of the main obstacles in establishing the straightforward linear relationship between angular speed $\dot{\theta}$ and in-cylinder pressure $p_g(\theta)$.

Since the mass torque T_m depends on design parameters of crankshaft mechanism it is quite predictive and can be calculated in advance. Relaying on this idea Moskwa suggested the method [6] in which the whole mass torque is replaced by the product of the constant moment of inertia and a new synthetic variable called synthetic angular acceleration. He used this method as a linearization technique for accessing the combustion information through measured angular acceleration. Therefore the term "synthetic", used in this paper, is inspired by the work of Moskwa and is an association on idea of eliminating the inertia effects from the measured angular speed signal.

Schagerberg [7] analysed the crankshaft model complexity influence on the estimation of combustion features using torque balance equation. In general, the more complex crankshaft model provide better results but the proper decision on how complex the crankshaft model should be, in order to give a satisfactory estimation of combustion features is related to the crankshaft modal shapes analysis [8].

The model used in this paper, is a multibody (lumped mass) based and takes the following matrix form:

$$\boldsymbol{J}\cdot\underline{\ddot{\theta}}+\boldsymbol{C}\cdot\underline{\dot{\theta}}+\boldsymbol{K}\cdot\underline{\theta}=\underline{T_g}(\theta)+\underline{T_m}\left(\theta,\dot{\theta},\ddot{\theta}\right)+\underline{T_l}(\theta)+\underline{T_f}(\theta) \tag{4}$$

where J, C and K are the inertia, torsional damping and stiffness N_L x N_L symmetrical matrices, respectively.

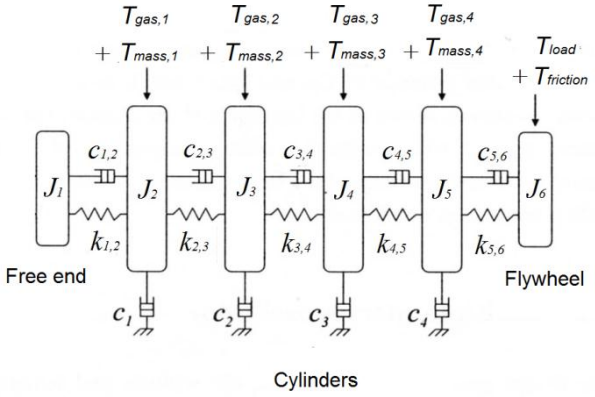

Figure 3 *A torsional crankshaft lumped mass model of the four cylinder engine*

The values, underlined in the equation (4), are the vectors whose elements respond to N_L individual lumped masses of the model. By assuming that the friction can be incorporated in damping loses, following variable can be defined:

$$T_{synth}(\theta)=\sum_{N}\left(\boldsymbol{J}\cdot\underline{\ddot{\theta}_{m*}}+\boldsymbol{C}\cdot\underline{\dot{\theta}_{m*}}+\boldsymbol{K}\cdot\underline{\theta_{m*}}-\underline{T_m}\left(\theta,\dot{\theta},\ddot{\theta}\right)\right) \tag{5}$$

This variable represents the estimate of the gas and the load torque sum and, knowing the parameters of the crankshaft model defined by eq. (4), can be calculated solely by means of measured crankshaft speed / acceleration (m* subscript in eq. (5)). The variable T_{synth} contains complete information on combustion process. Since the variations of this variable are more influenced by the combustion process than load variation, this variable is a good candidate for combustion features estimation. The drawback of this approach and its prerequisite is the necessity for crankshaft model parameter identification. The next step, needed for estimating combustion feature from this variable, is the establishment of a model which is able to accurately correlate T_{synth} and MFB50.

ANN STRUCTURE AS A BASE FOR MFB50 VIRTUAL SENSOR

The relationship between T_{synth} values and combustion feature like MFB50 is highly nonlinear and depends on several complex processes mainly the heat release and heat transfer process. Nonlinearities are introduced by various, engine specific, parameters and circumstances derived from combustion chamber design, cylinder filling-emptying processes, engine's working point, air-fuel ratio and so on.

The neural network models are featured by capabilities to establish functional approximation of the highly nonlinear correlated data. In fact, their structure mimics the massively parallel-distributed processing virtue of a brain [9] by using multiple interconnected processing units. One of the goals of this work is to accomplish ANN structured models being capable to execute fast enough to be implemented in available engine ECUs. Therefore the focus is

put on the RBF ANNs and Neuro-fuzzy based models, since they are able to achieve same or even better performance than widely used MLP networks, but with more compact structures.

Radial basis function networks, as shown on the Figure 4, have one hidden layer. The main processing units of this layer are the neurons with implemented activation function, which is often (as in this study) a Gaussian RBF. The RBF neural network is very well suited for multidimensional problems and is able to act as an MIMO (Multiple Input Multiple Output) system. The network k-th output is calculated as:

$$y_{k_{RBF}} = \sum w_{jk} \cdot e^{-\frac{\|x-c_j\|^2}{2\cdot\sigma_j^2}} \tag{6}$$

where w_{jk} are the weighing coefficients, c_j denotes the centre of the j-th Gaussian function, and σ_j its width. The learning method, used for the estimation of the RBF network weights and biases is based on the Orthogonal Least Squares algorithm (OLS).

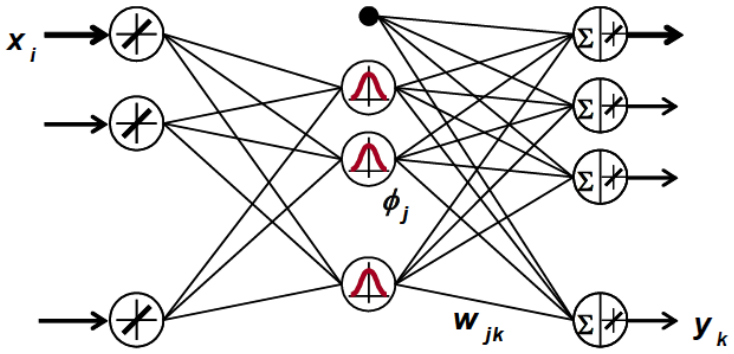

Figure 4 *The radial basis function ANN structure [11]*

By drawing the fuzzy models in a neural network based structure, hybrid Neuro-fuzzy (NF) models can be created [12].The advantage of local linear NF models, in an approximation of a nonlinear function, is their capability to model complex nonlinearities by superposition of several very simple models - linear functions. The first step in defining LLNF model is partitioning of the input vector $\underline{u}$ and placing, locally valid, linear models. Validity of each linear model $\mathrm{L_i}(\underline{u})$ is further defined by validation function $\Phi_\mathrm{i}(\underline{u})$.
The output of the LLNFM is defined as:

$$\begin{aligned} \hat{y} &= \sum_{i=1}^{M} L_i(\underline{u}) \cdot \Phi_i(\underline{u}) \\ \mathrm{L_i}(\underline{u}) &= \sum_{i=1}^{p} w_{i0} + w_{i1} \cdot u_1 + \cdots + w_{ip} \cdot u_p \end{aligned} \tag{7}$$

where *M* is the number of the local linear models and $\mathrm{w_{ij}}$ are the parameters of the *i*-th linear submodel; $\mathrm{u_1} \cdots \mathrm{u_p}$ are the elements of the input vector $\underline{u}$. The validity function, often used, is a normalised Gaussian function in the form:

$$\begin{aligned} \Phi_\mathrm{i}(\underline{u}, c_i, \sigma_i) &= \frac{\psi_i}{\sum_{k=1}^{M} \psi_k} \\ \psi_i &= \exp\left(-\frac{1}{2} \cdot \left(\sum_{j=1}^{p} \left(\frac{u_j - c_{ij}}{\sigma_{ij}} \right)^2 \right) \right) \end{aligned} \tag{8}$$

where c_{ij} is the Gaussian function centre coordinate and σ_{ij} individual standard deviation for the *j*-th input and *i*-th model partition (submodel).

Structure of LLNF model, described by the equations (7) – (8), is shown in the Figure 5. The training algorithm used, named Lolimot (Local Linear Model Tree), is introduced by Nelles [12].

In order to take into account the parameters, which significantly influence the combustion process, cycle averaged pressure in the intake manifold $\overline{p}_{im}$ and the cycle averaged crankshaft speed $\overline{n}_{eng}$ are added to the input vector which takes the form:

$$\underline{u}^{(i)} = [\underline{T}_{synth,map}^{(i)} \ \overline{n}_{eng,map}^{(i)} \ \overline{p}_{im,map}^{(i)}] \tag{9}$$

where (i) designates each engine cycle. All three signals, comprising the input vector, are mapped into the range [-1 1], as usual in the ANN input data preparation process.

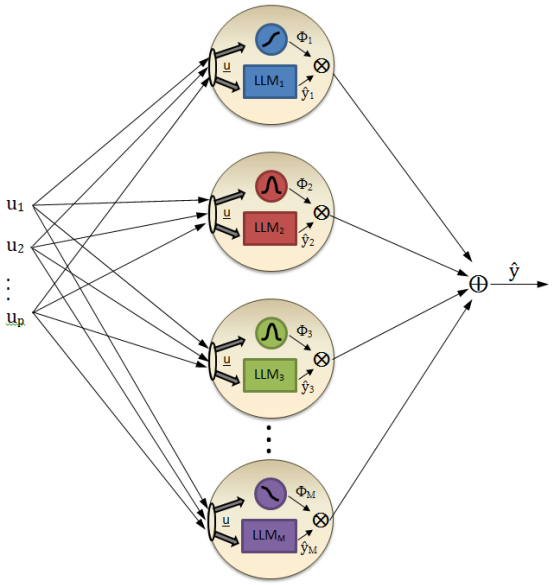

Figure 5 *The structure of the local linear Neuro-fuzzy model*

The RBF network is employed to form a MIMO system giving an output in the vector form with complete reconstruction of the mass fraction burned curve (eq. (6)). Since the LLNF model is simpler to employ as a MISO (Multiple Input Single Output) system, its output is defined as a single scalar - MFB50 combustion indicator:

$$\hat{y}_{LLNF}^{(i)} = MFB50^{i} \tag{10}$$

MEASUREMENT SETUP

The engine used, as an experimental object, is described in the Table 1. The identification of parameters of the crankshaft model requires measurement of the crankshaft angular speed. It was accomplished by means of optical incremental encoder (1º CA resolution), mounted at the free end of the crankshaft. Simultaneously, in-cylinder pressure was measured by means of piezoelectric, water cooled pressure sensor. Both signals, measured in angular domain, where crucial for preparing input (T_{synth}) and output (*MFB50*) training and test data sets for Neuro-fuzzy virtual sensor model.

Anticipated accuracy of LLNFM is related to the amount and the quality of the data acquired for its training and testing. The engine was equipped with the laboratory prototype of a variable induction system (VIS). This system [14] had an ability to influence the intake port airflow, when turned on, which consequently affected the combustion process. For that reason, this system was used in order to almost double the number of engine's working points by simply turning that system on (VIS-on) or off (VIS-off).

Table 1 *The engine data*

Manufacturer	DMB
Type	4 cylinder inline 4 stroke SI; 2 valves per cylinder
Firing sequence	1-3-4-2
Bore [mm]	80.5
Stroke [mm]	67.4
Conrod length [mm]	128.5
Piston pin offset [mm]	3.6
Compression ratio [-]	9.03

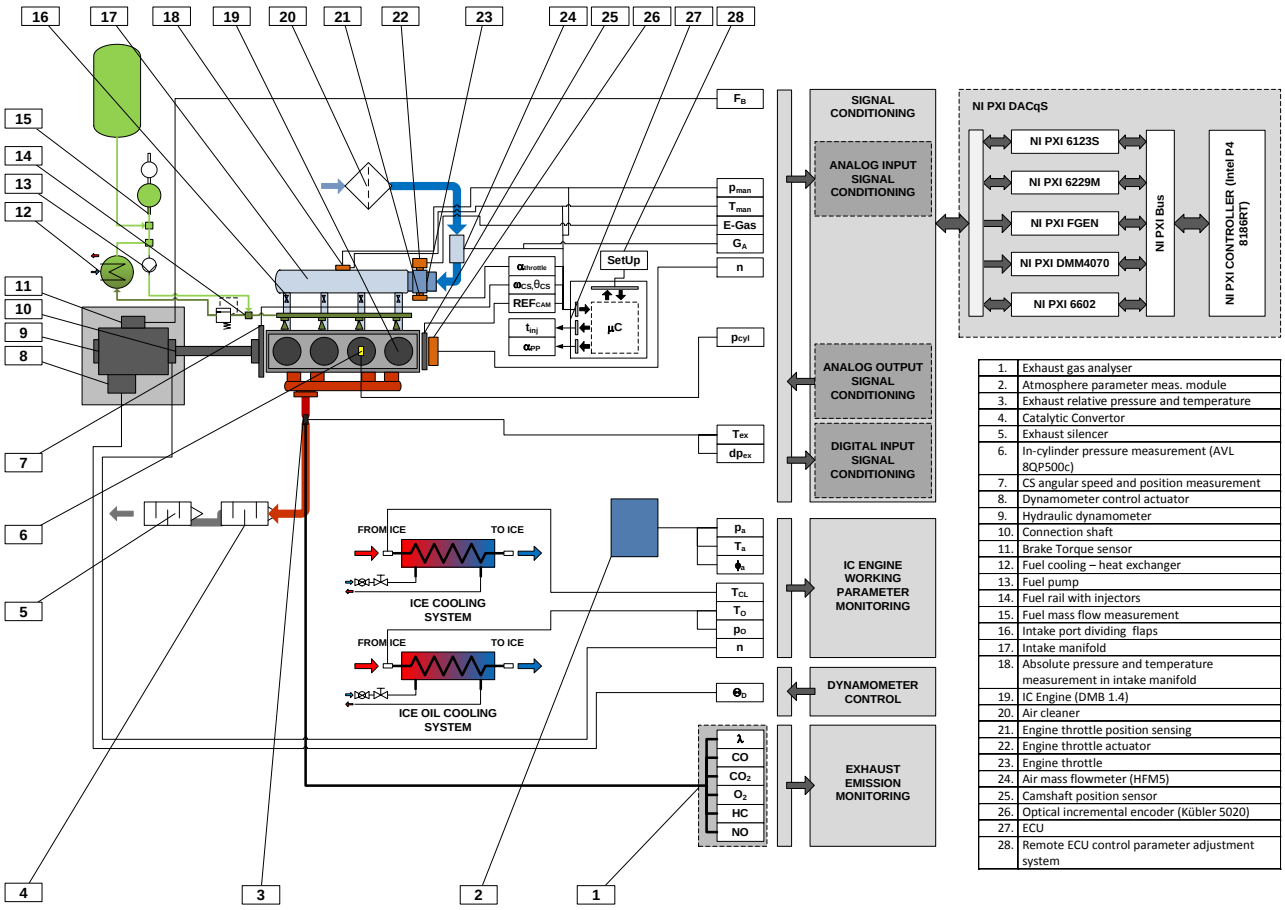

1.	Exhaust gas analyser
2.	Atmosphere parameter meas. module
3.	Exhaust relative pressure and temperature
4.	Catalytic Convertor
5.	Exhaust silencer
6.	In-cylinder pressure measurement (AVL 8QP500c)
7.	CS angular speed and position measurement
8.	Dynamometer control actuator
9.	Hydraulic dynamometer
10.	Connection shaft
11.	Brake Torque sensor
12.	Fuel cooling – heat exchanger
13.	Fuel pump
14.	Fuel rail with injectors
15.	Fuel mass flow measurement
16.	Intake port dividing flaps
17.	Intake manifold
18.	Absolute pressure and temperature measurement in intake manifold
19.	IC Engine (DMB 1.4)
20.	Air cleaner
21.	Engine throttle position sensing
22.	Engine throttle actuator
23.	Engine throttle
24.	Air mass flowmeter (HFM5)
25.	Camshaft position sensor
26.	Optical incremental encoder (Kübler 5020)
27.	ECU
28.	Remote ECU control parameter adjustment system

Figure 6 *The IC Engine test bed with the instrumentation and control systems*

Totally 141 engine's test points were recorded with 50 cycles each, which gave more than 7000 input-output pairs of data for neural network based model training and testing. Ought to mention that this number is not impressive in the world of IC engine neural models data gathering, but it was limited because of specific restrictions found on the engine used on a test bench.

Data analysis and preparation

Since the accuracy of measured signals has the key influence on usability of created models, full attention is paid for the correction of the measured angular speed due mechanical imperfections of measurement system [15], [16]. Measured in-cylinder pressure curves are corectly positioned in absolute pressure domen by means of methods described by Hohenberg [18] and Brunt in [19] which provided the pressure ofset values.

The TDC position and the compression ratio, as well, are the factors which largely affect the accuracy of all in-cylinder pressure derived conclusions. Correct TDC position and compression ratio are determined by the method described by Tazerout [20], which is based on the T-S (entropy - temperature) diagram peak shape and symmetry analysis. Because of its importance, determined TDC position is checked also by the thermodynamically based method, proposed by Tunestål [21] which confirmed a good agreement with the T-S shape & loop method (within 0.1º CA).

Correctly positioned in-cylinder pressure further provided the base for calculation of MFB curve and determination of MFB50 position for each of the measured engine cycles which will be used as targets in training and testing process of LLNFM. The calculation of the burn rate is closely related to the heat release and heat transfer process during combustion.The method proposed in [22] is simple, straightforward and an example of corect procedure for estimating the heat release curve. However, most of publications discussing the spark advance, MBT (Maximum Brake Torque) and MFB50 relations, as well as their conclusions, are based on Rassweiler & Whitrow (R&W) method for the burn rate calculation [23]. Therefore, the method used for MFB curves evaluation will be also based on R&W method, but slightly improved by Shayler [24].

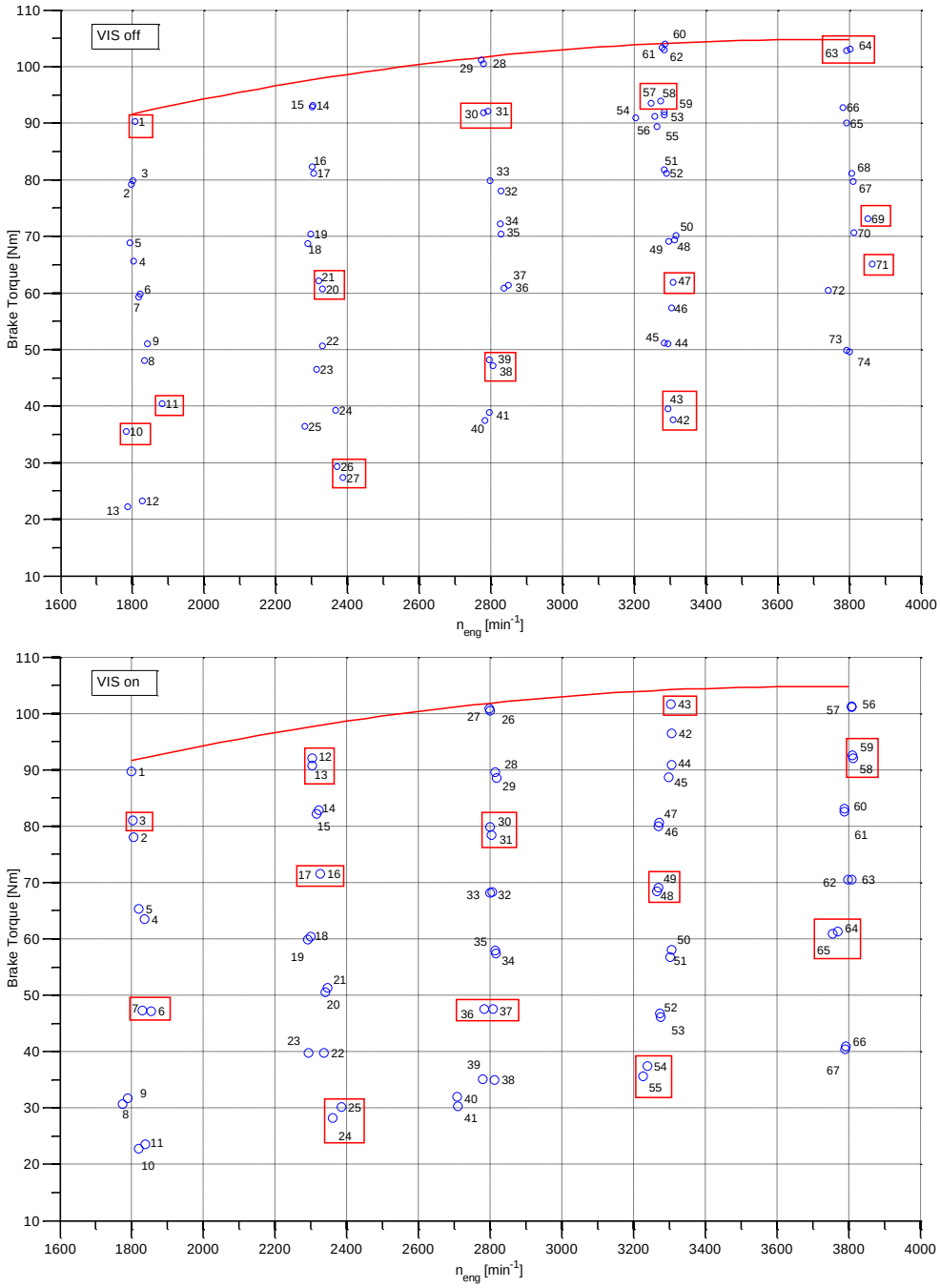

Figure 7 *The map of the recorded stationary engine regimes with VIS on (above) and VIS off (below). The regimes, marked with rectangles, are separated for NN training (cca. 30%). The rest of the data is used for model testing (cca. 70%).*

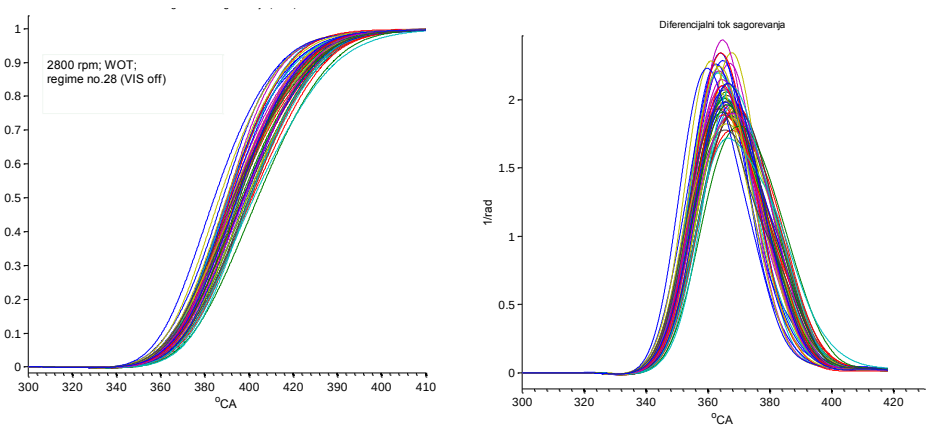

Figure 8 *Typical results of the MFB curve calculation (left) and its derivative (right); 50 consecutive cycles*

MODEL PARAMETER IDENTIFICATION

Rearrangement of the equation (4) and separation of terms in eq. (3) leads to second-order differential equation of motion of the crankshaft:

$$\boldsymbol{J}(\theta)\cdot\underline{\ddot{\theta}} = -\boldsymbol{C}\cdot\underline{\dot{\theta}} - \boldsymbol{K}\cdot\underline{\theta} + \underline{T_g}(\theta) + \underline{T_{m_2}}\left(\theta,\dot{\theta}\right) + \underline{T_l}(\theta) + \underline{T_f}(\theta) \tag{11}$$

where the varying inertia is the term multiplying $\ddot{\theta}$ in (3)

$$\boldsymbol{J}(\theta) = -\boldsymbol{J_A}(\theta) + \boldsymbol{m_B}r^2 + \underline{\boldsymbol{J}} \tag{12}$$

and the mass moment $\underline{T_{m_2}}$ is the part of eq. (3), which depends on the angular speed:

$$\underline{T_{m_2}}\left(\theta,\dot{\theta}\right) = -\frac{1}{2}\cdot\frac{d\boldsymbol{J_A}(\theta)}{d\theta}\cdot\dot{\theta}^2 \tag{13}$$

Equation (11) can be further transformed to the system of two first-order equations. The in-line four cylinder crankshafts can be modelled as a system of 6 lumped masses interconnected with torsional damper and spring elements, which is shown in the Figure 3. That in start gives 16 unknown parameters which should be identified (5 stiffness and 5 damping coefficients; 6 moments of inertia). By comparing the simulated ($\underline{\hat{\ddot{\theta}}_{sim}}$) and measured ($\underline{\ddot{\theta}_{meas}}$) angular acceleration error function $\mathcal{F}$ can be formulated:

$$\mathcal{F}\left(\underline{p_s}\right) = \left[\underline{\ddot{\theta}_{meas}} - \underline{\hat{\ddot{\theta}}_{sim}}\left(\underline{p_s}\right)\right]^T\cdot\left[\underline{\ddot{\theta}_{meas}} - \underline{\hat{\ddot{\theta}}_{sim}}\left(\underline{p_s}\right)\right] = \mathcal{E}^T\cdot\mathcal{E} \tag{14}$$

with $\underline{p_s}$ as a vector containing not yet identified parameters. This function can be successfully minimised by means of Levenberg-Marquardt algorithm. When the parameters of the crankshaft model are identified it is possible to apply eq. (5) and calculate the synthetic torque variable.

Examples of calculated signals T_{synth} are shown in the Figure 9 . The disturbances, which are noticeable on higher engine speed, especially on descending side of the signal, indicate that mass torque influence is not completely vanished. This is mainly a consequence of a fairly simple approach in the modelling of the friction torque. However, within the angular window in which combustion occurs, these anomalies are hardly visible. The focus of the analysing window is in 40° before and after TDC where the complete combustion mainly occurs.

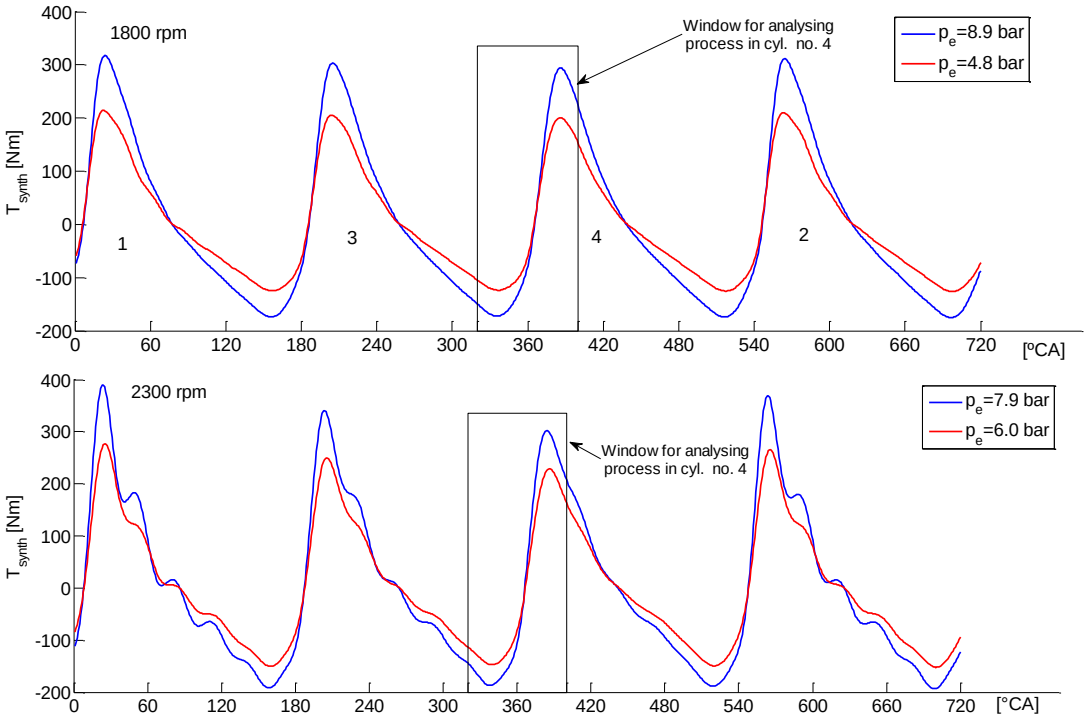

Figure 9 *An examples of calculated Tsynth on 1800 and 2300 rpm on full (blue) and partial load (red)*

The calculated T_{synth} values are further prepared for the placement in the ANN / LLNF input vector by mapping its input range to the interval [-1…1]. In order to identify the optimal structure of the RBF network, a series of numerical tests is conducted by changing the maximum number of neurons used $M \in \{7,14\}$, and the spread parameter (spread $\in [3 \ldots 10]$), defining the width of Gaussian RBF (see eq. (6)).

The key parameters, determining the performance of the LLNF model are the number of local linear models (neurons) M, and the Gaussian function width, given via parameter σ_L. In order to find the optimal values of these parameters several numerical tests were conducted by varying number M $\in [2 \ldots 7]$, and $\sigma_L \in [0.2 \ldots 0.5]$. The performance indicator used, was the standard deviation of MFB50 estimating error:

$$\sigma_{\Delta_{MFB50}} = \sqrt{\frac{1}{N-1} \cdot \sum_{N} \left(\Delta_{MFB50} - \overline{\Delta}_{MFB50}\right)} \tag{15}$$

where N is the number of input vectors available for training / validation (number of engine cycles). Estimating error is defined as:

$$\Delta_{MFB50} = MFB50_{sim} - MFB50_{measured} \tag{16}$$

It should be noted that the commonly used performance indicator – mean squared error (MSE), have values which are, more or less, halved when compared to $\sigma_{\Delta_{MFB50}}$. Therefore, the $\sigma_{\Delta_{MFB50}}$ parameter measures the performance of the model more strictly. Moreover, it is statistically significant parameter which can be usefully incorporated in the overall model performance analysis.

Testing the RBF network with the full length input vector containing T_{synth} with 81 elements (1°CA resolution on [-40…+40]°CA span around TDC), showed that this model is capable to reconstruct the MFB curve with a remarkable accuracy (see Figure 10).

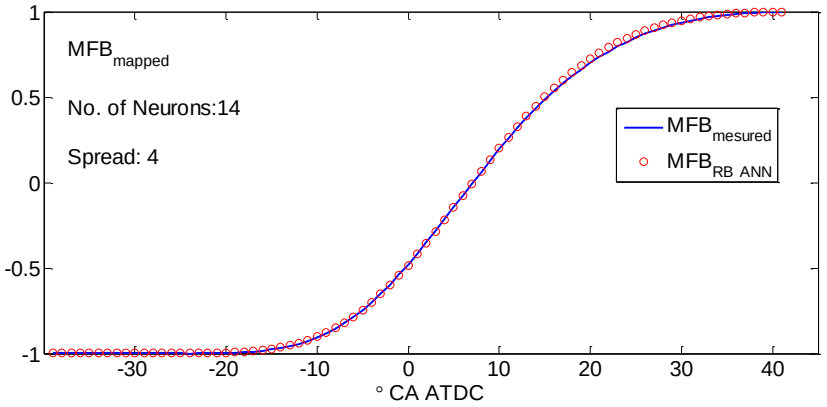

Figure 10 *The comparison of the measured (R&W) and simulated MFB curve with RBF ANN (one of the engine cycles from the test point No. 27)*

With the reduction of the input vector size, created RBF models can be executed faster, reducing CPU load. Therefore some further numerical experiments were conducted with shortened variants of the input vector element T_{synth}, by coarsening its angular resolution. For an example, if the angular resolution of the T_{synth} is reduced to 6° CA , size of the input vector $\underline{u}$ (eq. (9)), can be significantly reduced by employing 15 instead of 83 elements (13 × $T_{synth_{map}}$ + $\overline{n}_{eng,map}$ + $\overline{p}_{im,map}$). Tests with, this shorter variant of the T_{synth}, showed that the estimation of the MFB50 indicator, solely, can be achieved without significant reduction of estimation accuracy.

Some of the numerical tests of RBF ANN models are presented in Table 2. These results indicate that the smaller number of data points in T_{synth} can lead to better MFB50 estimation. The performance indicator $\sigma_{\Delta_{MFB50}}$ is calculated over test data set, by using a model trained on data set which comprises only 30% of the complete data set. This indicates that the models created have a good performance and generalization capabilities. The results of numerical tests on LLNF models are shown in Table 3. It is indicative that the LLNFM model can achieve very similar performance, compared to RBF ANN, but with smaller number of sub models, i.e. neurons.

Cycle-by-cycle variations are common in SI engines. Pipitone [25] concluded, that combustion features, extracted in cycle-by-cycle manner and used as an input in a spark advance control system, can cause very large fluctuations of this control variable (±10°CA). In order to avoid this, and provide the spark advance control system with the more stable combustion indicator, its value should be averaged.

Table 2 *The partial results of the numerical tests of different RBF ANN model configurations – values of* $\boldsymbol{\sigma_{\Delta_{MFB50}}}$ *on test data set (5000 cycles) in °CA*

T_{synth} angular resolution [°CA]	No. of neurons	Spread	$\sigma_{\Delta_{\mathrm{MFB50}}}$
1	14	4	0.356
	21	10	**0.319**
	43	8	0.411
	81	8	0.654
6	7	5	0.545
	14	8	**0.374**

Table 3 *The results of the numerical tests of different LLNF model configurations – values of* $\boldsymbol{\sigma_{\Delta_{MFB50}}}$ *on test data set (5000 cycles) in °CA (* $\boldsymbol{T_{synth}}$ *resolution is 6° CA)*

M↓ σ_L→	0.2	**0.24**	0.3	0.4	0.5
2	0.400	0.405	0.414	0.445	0.447
3	0.392	0.382	0.391	0.385	0.496
4	0.369	0.357	0.419	0.353	0.576
5	0.353	**0.332**	0.389	0.351	0.610
6	0.581	0.340	0.452	0.379	0.590
7	0.597	0.341	0.486	0.385	0.585

Pipitone also showed that for the MFB50 indicator, the minimum number of engine cycles for stable indicator evaluation is strongly dependent on IMEP COV (Indicated mean effective pressure coefficient of variation), with the conclusion that the mean value of minimum number of cycles is around 14. Having this in mind, resulted output vector of both RBF and LLNF models is averaged by moving average filter (14 cycle width), and performance indicators are calculated over this smoothed MFB50 output.

A variation of the error Δ_{MFB50}, in estimating the MFB50 combustion indicator on the test data set, for some RBF ANN and LLNF models, is shown in the Figure 11 and Figure 12, respectively. It is clear that the performance of the both model structures used, suffers on some cycles with MFB50 estimation error exceeding more than 1°CA. Most of these cycles belong to the partial load regimes, driven with the leaner air-fuel mixture, where partial combustions and misfires are not uncommon. This implies that the air to fuel ratio (AFR), as an additional element in the neural network input vector $\underline{u}$, could improve the model performance.

Pipitone also concluded that acceptable variation of an estimated MFB50 indicator can be as high as ±1. 63°CA in order to maintain the spark advance within the ±1.8°CA, which consequently influences the efficiency loss with an acceptable mean of 0.2%. In order to evaluate the performance of the proposed models, variation of the estimated MFB50 values should be compared with that limits. By assuming that the almost whole span of estimated values is in the range of (2…3) × $\sigma_{\Delta_{MFB50}}$, an acceptable variation of the MFB50 estimation should be:

$$\sigma_{\Delta_{MFB50}} < 0.54° \, CA \tag{17}$$

which means that the both model structures can provide models with the required accuracy (see Table 2 and Table 3), and can be potentially used in closed loop spark advance control systems, even without discussing the above mentioned misfire or partial combustion problems.

The execution time of the MFB50 virtual sensor model comprised of T_{synth} calculation and MFB50 combustion indicator estimation is, along with its accuracy, a crucial feature which determines the possibility of the real-time in-vehicle application. Therefore it is interesting to make some basic benchmark of these models on two distinctive CPUs: PC and automotive microcontroller (μC) CPU.

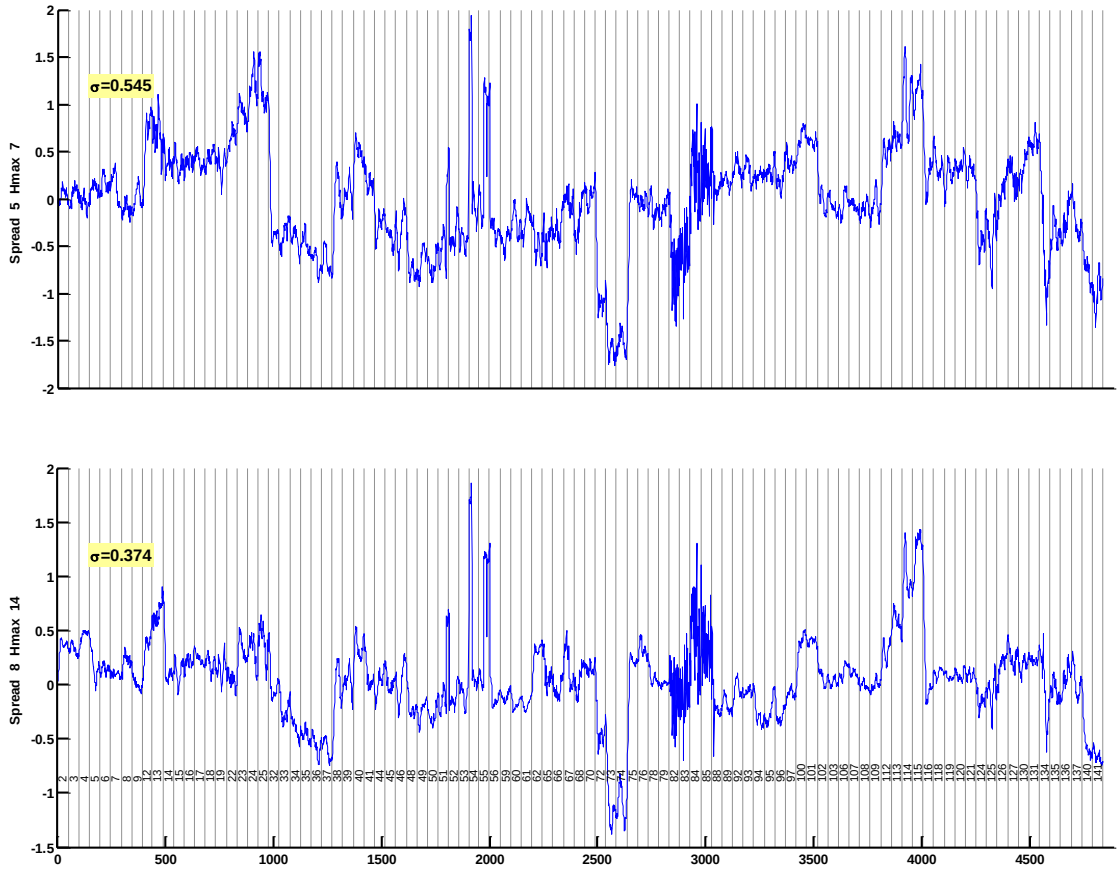

Figure 11 Δ_{MFB50} *variation on the test data set [°CA], RBF ANN;* T_{synth} *resolution is 6° CA*

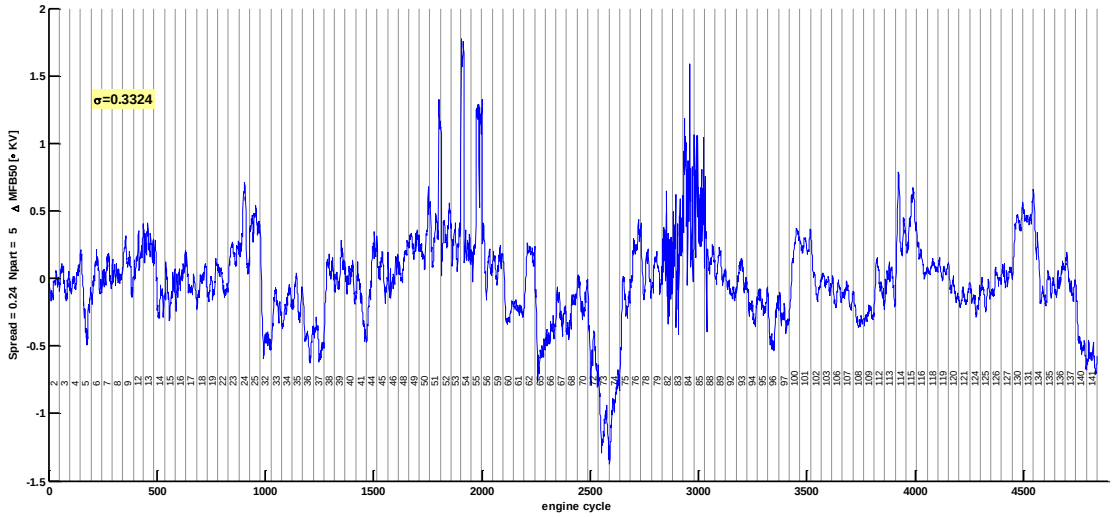

Figure 12 Δ_{MFB50} *variation on the test data set [°CA], LLNFM* $\sigma_L = 0.24$*, M=5;* T_{synth} *resolution is 6° CA*

The most compact model, satisfying accuracy requirements defined by eq. (17), is LLNFM with 5 local linear models which expect input vector with 15 elements. The coefficients of this model are stored in 5×16 matrix of double precision numbers. The model execution, i.e. single MFB50 estimation on PC computer with an Intel I7-920 (3.3 GHz) processor, takes roughly 7 µs (or less) per function call. This execution time is achieved with the model compiled and executed under the non-real-time PC Windows 7 OS.

One of the typical engine ECU is often based on the Freescale MPC500 series µCs. Taken for an example, MPC565 has an CPU which the maximum running speed of 56 Mhz. When compared, via commonly used CPU speed unit (so called MIPSs), this µC should have more than 150 times slower execution speed. Quite opposite, when optimised and compiled for embedded application (Freescale CodeWarrior compiler), and executed in real-time conditions, the execution speed of "benchmark" LLNF model was only twice slower than on PC, i.e. 13.6 µs.

This can be explained by the high utilisation of the μC CPU in a real-time task, which differs largely from the working conditions of the ordinary PC with non-real-time OS.

The complete execution time of the proposed MFB50 virtual sensor includes the CPU time for T_{synth} and calculated MFB50 averaging. Even if that time is 100 times larger than benchmarked values, the total execution time is acceptable for ECU μCs like MPC500, which are already in the category of obsolete units (compared to the capabilities of the actual Freescale MPC55xx series, or similar μCs from other manufacturers).

Whereas the results showed are promising, further research could be focused on additional input vector size reduction which can lead to even more compact and faster models with the same or even improved performance. This input vector size reduction should rely on extraction of the most important information content from the T_{synth} variable. Some techniques for data size reduction, like one based on the Mutual Information concept, seems particularly promising and applicable [27].

CONCLUSIONS

In order to accomplish the optimal combustion efficiency, a modern engine control systems requires a closed loop spark advance control which relies on accurate information on combustion process. Whereas the in-cylinder pressure based methods are able to provide this information, an alternative approach, based solely on the crankshaft angular speed measurements and its processing, is suggested. The proposed sensing system estimates MFB50 combustion feature by calculating so called synthetic torque, and transforming it to MFB50 value through nonlinear estimator based on the artificially neural network structured models like RBF ANNs or LLNF models.

The calculation of the synthetic torque is based on the identified parameters of a high fidelity calibrated dynamic model of the crankshaft. The synthetic torque signal contains high quality information on the combustion process with negligible mass torque influence thus simplifying the combustion process information extraction. The neural network input vector, based on the synthetic torque signal, the averaged cycle engine speed and the intake manifold pressure, provides enough information for the highest quality training of the RBF or LLNF models.

Trained with the 30% and tested on 70 % of acquired experimental data, both RBF and LLNF models demonstrated very good performance in estimating the MFB50 with excellent generalization capabilities. Furthermore RBF models demonstrated a capability to estimate the shape of the whole MFB curve. The testing of the models showed that they are prone to generate increased errors in the MFB50 estimation on low load or idle engine regimes, mainly because of a misfire and partial combustion caused by leaner air-fuel mixture used. Despite this fact, designed LLNF and RBF models outperform the minimum allowable error variation and provide acceptable inputs for the closed-loop spark advance control system.

Compared to RBF, LLNF models are able to provide the same performance with more compact structure and smaller number of neurons. Since this affects their execution speed, LLNF models are more appropriate for the implementation in the engine ECUs.

The reduction of the input vector size, by reducing the angular resolution of the synthetic torque variable, enabled the compact design of the LLNF model with only 5 neurons. Further reduction of the neural network structure input vector, based on the information content extraction, could lead to the additional model size reduction and processing requirements which can be even more acceptable to the modern engine control units.

ACKNOWLEDGMENTS

The authors would like to thank the Freescale Semiconductor for providing the CodeWarrior Professional Development Suite for MPC5xx microcontroller platforms.

REFERENCES

[1] *CO2 Emissions from Fuel Combustion 2011 - Highlights*-. Paris: International Energy Agency (IEA), 2011.
[2] J. B. Heywood, *Internal combustion engine fundamentals*. McGraw-Hill, 1988.
[3] M. Bargende, “Schwerpunkt-Kriterium und automatische Klingenerkennung Bausteine zur automatischen Kennfeldoptimierung bei Ottomotoren,” *MTZ*, vol. 56, no. 10, pp. 632–638, 1995.

[4] A. Beccari, S. Beccari, and E. Pipitone, “An Analytical Approach for the Evaluation of the Optimal Combustion Phase in Spark Ignition Engines,” *J. Eng. Gas Turbines Power*, vol. 132, no. 3, pp. 032802–11, Mar. 2010.
[5] H. Maass, *Kr ft e, Momente und deren Ausgleich in der e rbrennungskraftmaschine*. Wien [u.a.]: Springer, 1981.
[6] J. J. Moskwa, W. Wang, and D. J. Bucheger, “A New Methodology for Use in Engine Diagnostics and Control, Utilizing ‘Synthetic’ Engine Variables: Theoretical and Experimental Results,” *Journal of Dynamic Systems, Measurement, and Control*, vol. 123, no. 3, p. 528, 2001.
[7] S. Schagerberg and T. Mckelvey, “Instantaneous Crankshaft Torque Measurements - Modeling and Validation,” SAE International, Warrendale, PA, 2003-01-0713, Mar. 2003.
[8] F. Ponti, “Development of a Torsional Behavior Powertrain Model for Multiple Misfire Detection,” *J. Eng. Gas Turbines Power*, vol. 130, no. 2, p. 022803, 2008.
[9] S. S. Haykin, *Neural networks: a comprehensive foundation*. Macmillan, 1994.
[10] M. T. Hagan, Demuth, and Beale, *Neural Network Design*. Brooks/Cole, 1996.
[11] K. L. Priddy and P. E. Keller, *Artificial neural networks: an introduction*. SPIE Press, 2005.
[12] O. Nelles, *Nonlinear system identification: from classical approaches to neural networks and fuzzy models*. Springer, 2001.
[13] N. Müller, M. Hafner, and R. Isermann, “A Neuro-Fuzzy Based Method for the Design of Combustion Engine Dynamometer Experiments,” SAE International, Warrendale, PA, 2000-01-1262, Mar. 2000.
[14] M. Tomić, S. Petrović, S. Popović, and N. Miljić, “Dual Port Induction System for DMB 1.4MPI Engine,” in *DEMI 2011 - Proceedings*, Banja Luka, 2011.
[15] U. Kiencke and R. Eger, *Messtechnik: Systemtheorie für Elektrotechniker*. Springer, 2008.
[16] H. Fehrenbach, C. Hohmann, T. Schmidt, W. Schultalbers, and H. Rasche, “Kompensation des Geberradfehlers im Fahrbetrieb,” *MTZ*, vol. 63, no. 7/8, pp. 588–591, 2002.
[17] M. F. J. Brunt and A. L. Emtage, “Evaluation of Burn Rate Routines and Analysis Errors,” SAE International, Warrendale, PA, 970037, Feb. 1997.
[18] G. K. Hohenberg, “Basic findings obtained from measurement of the combustion process,” Melbourne, 1982.
[19] M. F. J. Brunt and C. R. Pond, “Evaluation of Techniques for Absolute Cylinder Pressure Correction,” SAE International, Warrendale, PA, 970036, Feb. 1997.
[20] M. Tazerout, O. Le Corre, and P. Stouffs, “Compression Ratio and TDC Calibrations Using Temperature - Entropy Diagram,” SAE International, Warrendale, PA, 1999-01-3509, Oct. 1999.
[21] P. Tunestål, “TDC Offset Estimation from Motored Cylinder Pressure Data based on Heat Release Shaping,” *Oil & Gas Science and Technology – Revue d’IFP Energies nouvelles*, vol. 66, no. 4, pp. 705–716, Oct. 2011.
[22] M. Tomic, S. Popovic, N. Miljic, S. Petrovic, M. Cvetic, D. Knezevic, and Z. Jovanovic, “A quick, simplified approach to the evaluation of combustion rate from an internal combustion engine indicator diagram,” *Thermal Science*, vol. 12, no. 1, pp. 85–102, 2008.
[23] G. M. Rassweiler and L. Withrow, “Motion Pictures of Engine Flames Correlated with Pressure Cards,” SAE International, Warrendale, PA, 380139, Jan. 1938.
[24] P. J. Shayler, M. W. Wiseman, and T. Ma, “Improving the Determination of Mass Fraction Burnt,” SAE International, Warrendale, PA, 900351, Feb. 1990.
[25] E. Pipitone, “A Comparison Between Combustion Phase Indicators for Optimal Spark Timing,” *Journal of Engineering for Gas Turbines and Power*, vol. 130, no. 5, p. 052808, 2008.
[26] M. Schmidt, F. Kimmich, H. Straky, and R. Isermann, “Combustion Supervision by Evaluating the Crankshaft Speed and Acceleration,” SAE International, Warrendale, PA, 2000-01-0558, Mar. 2000.
[27] F. Heister, “Nonlinear feature selection using the general mutual information,” Doctoral Thesis, Johann Wolfgang Goethe-Universität, Frankfurt am Main, 2008.